Journal of Metals, Materials and Minerals, Vol. 31, No. 4, pp. 102-107, 2021

Stress softening characteristics of thin monoholar rubber flat slab

Kulyuth BOONSENG[1,*], Chatchai WAIYAPATTANAKORN[2], and Prayoon SURIN[1]

[1] *Faculty of Engineering, Pathumwan Institute of Technology, Bangkok, 10330, Thailand*
[2] *Independent Academic, Bangkok, 10210, Thailand*

***Corresponding author e-mail:** kulyuth.bo@skru.ac.th

Received date:
1 August 2021
Revised date
9 October 2021
Accepted date:
18 October 2021

Keywords:
Thin Monoholar;
Elastomeric material;
Stress softening;
Permanent set strain;
Hysteresis loss energy

Abstract

Thin monoholar rubber flat slab gives rise to unconventional mechanical properties under tension loading not found in thin solid rubber flat slab. However there has been no proper report on its stress softening characteristics. Stress softening is an important phenomenon occurring in all elastomeric materials under cyclic tension loading. Parameters pertinent to stress softening investigated in this research are stress-strain characteristics, permanent set strain and hysteresis loss energy of the thin monoholar rubber flat slab in comparison with the thin solid rubber fat slab when undergoing 7 cycles of stretching. Noticeable differences of stress-strain hysteresis loops diminution of the thin monoholar rubber flat slab and the solid rubber flat slab have been observed. However difference in stress softening between both types of flat slab is not so pronounced. The monoholar rubber flat slab specimens have larger permanent set strain and hysteresis loss energy diminution compared with those of the solid rubber flat slab. If both permanent set strain and hysteresis loss energy diminution have been properly accounted for, stress softening may not be a matter of great concern when the monoholar rubber flat slab is adopted in practical applications.

1. Introduction

Technological advancement of today's world has fueled the demand for materials that are versatile, lightweight, load-bearing and heat resistant. Special properties are necessary for specific applications such as the aviation industry, energy industry, petrochemical industry, electronic industry, etc [1]. Natural materials cannot meet certain unusual requirements completely. Generally speaking, properties of typical materials depend on their chemical composition and microstructures [2]. To improve mechanical properties of the materials in use, various methods have been developed, such as friction welding [3], friction stir welding [4], heat treatment [5], composite materials [6] or even inventing smart material [7].

Over the past decade, researchers have been interested in developing materials by means of the cellular structure which could yield remarkable mechanical properties [1,2,8-14]. Cellular structure materials' functionality relies on elastic instabilities, such as the quasi-2D slabs perforated with a square array of holes [4,6,15-18]. It is well known that certain visualisable physical characteristics of the material affect its mechanical properties, even when using the same chemical composition [14,19-23]. The thin monoholar flat slab is another form of cellular structure employing a square array of equal sized circular holes [8,9,16]. It is a promising challenge and a trend of future research [1,15].

In the authors' previous work [16] it has been found that under moderate uniaxial tension loading stress-strain hysteresis loops of the monoholar rubber flat slab, a form of cellular structure, are larger than that of the solid rubber flat slab, showing a greater loss of energy resulting in greater energy absorption than the solid rubber flat slab. The monoholar rubber flat slab appears with greater stiffness to tension at moderate level of loading compared with the solid rubber flat slab. Both phenomena are likely due to elastic instability present in the monoholar rubber flat slab but not discernible in the solid rubber flat slab. This benefit of adopting repeated pattern or cellular structure is in accordance with most work reported in the literature [11,17-25]. The monoholar rubber flat slab may be an essential part of sport shoes or some soft robot arms, both of which will unavoidably face cyclic tension loading. It is thus worth investigating on the softening characteristics to obtain more knowledge for the best possible performance of the material. However reports on stress softening of elastomeric materials with cellular structure have not been found in the literature.

In many real world applications of elastomeric materials cyclic tension loading is inevitable. Knowledge and understanding of stress softening of elastomeric materials with cellular structure will benefit the design of material for many applications in various fields [14,26-30]. Recently there have been a few reported investigations concerning the Mullin's effect or stress softening of elastomeric materials with emphasis on the use of some novel types of fillers [31-33]. Their interests are different from what this research is intent on. Herein the emphasis is on possible added softening due to adopting certain repeated geometric pattern that alter visualizable physical characteristics of the thin rubber flat slab. Parameters of interest in the experimental investigation are stress-strain characteristics, permanent set strain and hysteresis loss energy, all of which are parameters pertinent to stress softening, of the thin monoholar

rubber flat slab in comparison with the thin solid rubber flat slab when undergoing 7 cycles of stretching. In the next section description of the experimentation is presented.

2. Experimentation

The experiments to be performed are those of cyclic uniaxial tensile loading test of both the solid rubber flat slab (SFS) (the referenced specimen) and the monoholar rubber flat slab (MFS) (the investigated specimen). This research has opted for a compounded rubber made of Standard Thai Rubber (STR20) 40 phr, Butadiene Rubber 60 phr, silica 50 phr and other compounds used in the shoe industry. The cellular structure of interest herein is the monoholar array. This is because of its construction simplicity [26]. Material preparation is as stated in [16]. Both types of specimens have been tested for hardness. The figure for the MSF is 70.00 ± 1.22 and that of the SFS is70.40 ± 0.55. Figure 1 depicts geometries of both the solid and monoholar flat slabs employed in the experiment. Both specimens are different in physical structure at the macro level. All dimensions are in millimeter. Both types of flat slabs are 1 mm thick. They are hence thin flat slabs. The experimental setup is as follows: Tensile properties are to be tested uniaxially using a universal testing machine (UTM), Narin Universal Testing Machine Model NRI-T500-20B. Stress softening are to be observed by pulling the specimens to 100 percent elongation, then the specimen is allowed to shrink back to its initial state. This is as a consequence of the finding in [16] that the MSF is capable of demonstrating unusual stress-strain characteristic under moderate tension loading. Further test has found that the MSF can cope with up to around 180% elongation beyond its original state. The tension loading action is to be performed for 7 cycles [11]. Each specimen is pulled at the rate of 500 mm/min at room temperature (25 ± 2°C) according to ASTM D412. Five specimens are to be tested and results are averaged to yield a reported value. Maximum stress of each cycle is recorded thus stress softening percentage can be calculated by Equation (1).

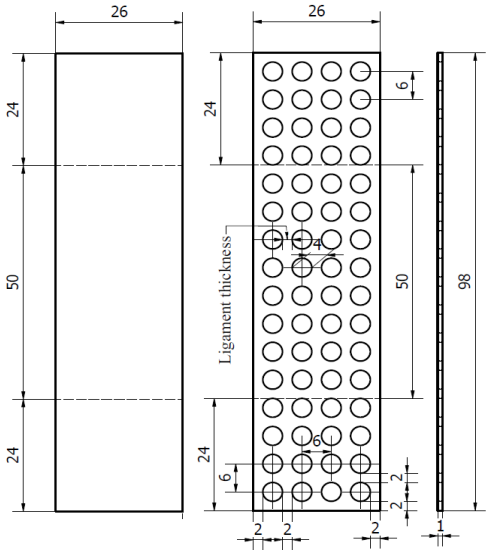

Figure 1. Specimen geometries (all dimensions are in mm) (a) Solid rubber flat slab (SFS), and (b) Monoholar rubber flat slab (MFS).

$$\textit{Stress softening percentage (\%)} = \frac{T_i}{T_1} \times 100 \quad (1)$$

where T_1 (MPa) is the maximum elongated stress in the first extension cycle and Ti (MPa) is the maximum elongated stress in the 1st -7th extension cycles.

Hysteresis loss energy can also be calculated by the use of Equation (2).

$$\textit{Hysteresis loss energy } (kJ{\cdot}m^{-2}) = \Delta L - \Delta U \quad (2)$$

where ΔL is the area under the graph between the stress (MPa) and the displacement (mm) during stretching ($kJ{\cdot}m^{-2}$). ΔU is the area under the graph between the stress (MPa) and the displacement (mm) during retraction ($kJ{\cdot}m^{-2}$).

3. Results and discussion

Both the MFS and SFS specimens have been subjected to 7 cycles of stretching in order to investigate their stress-strain characteristics, permanent set strain and Hysteresis loss energy. Detailed description of important results and discussion are as follows.

3.1 Stress-strain characteristics

3.1.1 Cyclic loading stress-strain hysteretic characteristics

Figure 2 shows the cyclic loading stress-strain hysteretic characteristics of the MFS and the SFS specimens. The hysteresis loops of both types of specimens, Figures 2(a) and 2(b), become smaller for successive loading cycles at a given displacement of 50 mm. (a given constant strain). This is an indication of the occurrence of stress softening under cyclic tension loading. It can be seen that the MFS stress-strain hysteresis loops, Figures 2(b), are larger than that of the SFS, Figures 2(a). Consider Figure 2(b) it is apparent that differences of the first cycle maximum stress and the successive cycles are larger than that of Figure 2(a). This is an evidence that there is stronger softening of the MSF specimens in comparison with the SFS specimens. This is likely a result of the presence of the spatial voids due to the patterned array of equal sized circular holes (monoholar pattern). The spatial voids cause shortening or breaking of molecaular chains, thus complete recovery to original state is not possible. The voids or the rubberless areas limit the extent or the length of the molecular chains thus cross linking or entanglement among molecular chains may not be as perfect as that of the whole piece of rubber. This is how slippage or breaking of molecular chains occurs more easily.

3.1.2 Stress-strain at 100% elongation

Elongated stress-strain characteristics of the MFS and SFS in this research confirm the authors' previous results [16] that greater stress is required for the same strain level in the case of the MFS. Of interest herein is the difference of the maximum stress at a given displacement of 50 mm of the first cycle and successive loading cycles, an indication of softening phenomenon. Visual comparison of Figures 3(a) and (b) clearly shows that the differences of the maximum

stress at a given displacement of the first cycle and successive loading cycles of the MFS are larger than that of the SFS. It thus confirms that the MSF exhibits greater stress softening than the SFS. This is also a result of shortening or breaking of molecular chains due to the spatial voids of the monoholar pattern.

3.1.3 Maximum Stress and Stress softening

Maximum stress values at 100% elongation stretch for 7 loading cycles of both the MFS and SFS are summarized in Table 1. Diminution of maximum stress values is summarised in Table 2 and also presented graphically in Figure 4. It is evidenced that there is a clear difference in the maximum stress between both types of specimens. It is also visibly observed that the red doth of the MFS has greater drop of maximum stress than that of the black curve of the SFS, which is a confirmation of stronger softening of the MFS. Calculation of stress softening percentage (according to Equation (1) in subsection 2.2) plotted in Figure 5 shows discernible difference in stress softening between the MFS and SFS specimens. The softening gap of the MFS and the SFS visible in Figure 5 begins from the second loading cycle and becomes larger from the third cycle to the fifth cycle. The widest gap is at cycle number 4 with the difference of around 1.8%. The softening of the SFS drops down to about the same level as that of the MFS from the sixth cycle onward which is typical of most softening phenomena in elastomeric materials [34-36]. The greater stress softening of the MFS specimens is likely a result of the presence of spatial voids, all circular holes of the monoholar pattern. Some of the voids cause shortening or breaking of the molecular chains, as a result of having more limited space for rubber compound molecular chains to extend, entangle or crosslink with one another. This is likely to further promote slippage of the crosslink or breaking up of molecular chains both of which are responsible for softening of elastomeric materials [37]. Hence after being stretched a few times softening observed in the MFS is discernibly stronger than that of the SFS.

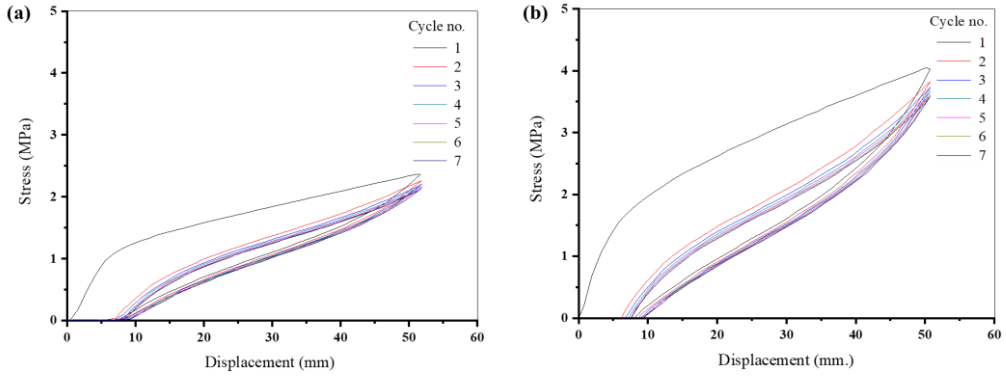

Figure 2. Hysteretic characteristics under 7 cycles of cyclic tension loading (a) Solid rubber flat slab (SFS) (b) Monoholar rubber flat slab (MFS)

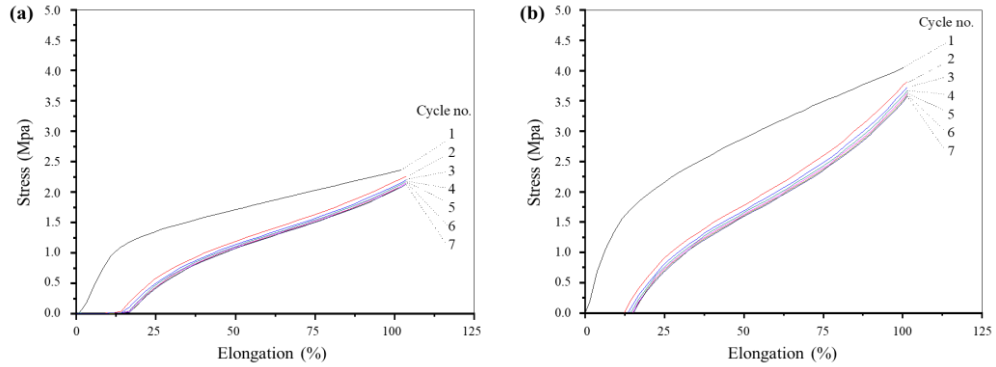

Figure 3. Stress-strain under 7 cycles of cyclic tension loading (a) Solid rubber flat slab (SFS) (b) Monoholar rubber flat slab (MFS).

Table 1. Maximum stress under 7 cycles of cyclic tension loading

Cycle no.	Maximum stress (MPa)	
	SFS	MFS
1	2.39 ± 0.033	3.89 ± 0.167
2	2.26 ± 0.010	3.67 ± 0.124
3	2.20 ± 0.019	3.53 ± 0.165
4	2.19 ± 0.038	3.50 ± 0.153
5	2.15 ± 0.015	3.47 ± 0.139
6	2.12 ± 0.031	3.46 ± 0.132
7	2.13 ± 0.013	3.48 ± 0.150

Table 2. Diminution of maximum stress.

Cycle no.	Maximum stress (MPa)	
	SFS	MFS
1	0	0
2	0.13	0.22
3	0.06	0.14
4	0.01	0.03
5	0.04	0.02
6	0.03	0.02
7	-0.01	-0.02

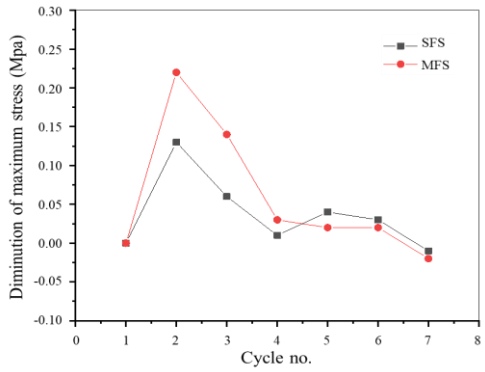

Figure 4. Diminution of maximum stress under 7 cycles of cyclic tension loading of solid rubber flat slab (SFS) and monoholar rubber flat slab (MFS).

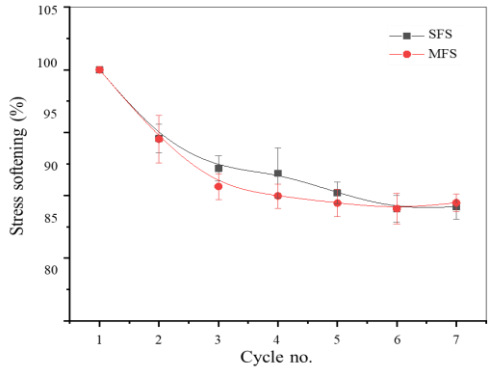

Figure 5. Stress softening percentage under 7 cycles of cyclic tension loading of solid rubber flat slab (SFS) and monoholar rubber flat slab (MFS).

3.2 Permanent set strain

Permanent set strain refers to the residual extension remaining after a material sample is stretched and released [38-39]. Figure 6 shows a convex curve of permanent set strain of the MFS whereas that of the SFS is rather flat. It is a result of greater drop in maximum stress of the subsequent loading cycles that eventually flattens off after the sixth cycle. This is in accordance with the stress softening percentage plot in Figure 5. It is evidenced from Figure 6 that permanent set strain of the MFS is greater than that of the SFS. Differences of permanent set strain of both types of specimens range from 4.16% to 5.75%. This is again a consequence of the shortening or breaking of the molecular chains due to the presence of the spatial voids in the MFS. Shorter or broken molecular chains disable complete recovery of the original state of the MFS. Residual strain or permanent set strain of the MFS is therefore greater after being stretched. The MFS is more susceptible to being damaged by cyclic tension loading than the SFS due to its elastic stiffness reduction as a result of greater stress softening.

3.3 Hysteresis loss energy

Figure 7 shows that hysteresis loss energy (according to Equation 2) of the MFS is greater than that of the SFS. Both curves are so similar with just an approximate offset of about 6.2 kJ·m^{-2}. The greatest difference of the first cycle is about 23 kJ·m^{-2}. The sharp drop of hysteresis loss energy in the subsequent cycles is noticeably more pronounced for the MFS, particularly the drop of the second loading cycle. The offset values of the subsequent cycles are not so different because after the second loading cycle the drop of hysteresis loss energy of both types of specimens are more or less the same. The offset of both curves is simply because the stress-strain hysteretic characteristics of the MFS yield larger hysteresis loops than that of the SFS, a consequence of elastic instability arising from the presence of the spatial voids in the MFS [16]. The MFS is thus more susceptible to being damaged under cyclic tension loading.

Of greater interest is the sharp drop or diminution of hysteresis loss energy under 7 cycles of cyclic tension loading of both types of specimens. It is evidenced from Table 3 that the MSF exhibits greater diminution of hysteresis loss energy. This means that reduction in the MFS' elastic stiffness is greater than that of the SFS'.

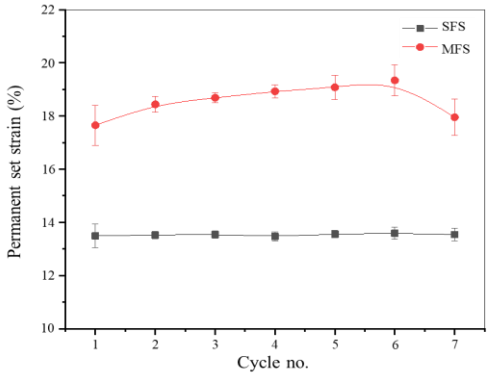

Figure 6. Permanent set strain of solid rubber flat slab (SFS) and monoholar rubber flat slab (MFS).

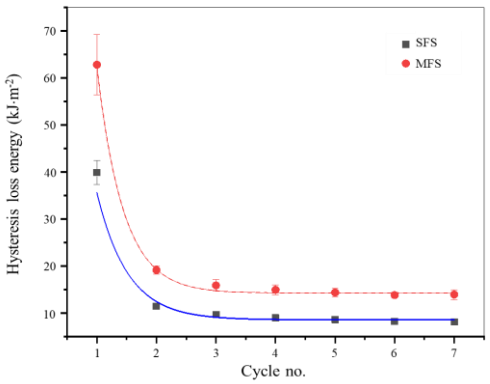

Figure 7. Hysteresis loss energy of solid rubber flat slab (SFS) and monoholar rubber flat slab (MFS).

Table 3. Diminution of hysteresis loss energy under 7 cycles of cyclic tension loading.

Cycle no.	Diminution of hysteresis loss energy (MPa)	
	SFS	MFS
1	0	0
2	28.42	43.62
3	1.73	3.27
4	0.73	0.94
5	0.36	0.58
6	0.38	0.55
7	0.09	-0.13

4. Conclusions

Knowledge of stress softening characteristic is essential for safe and effective utilization of elastomeric materials in applications that cyclic tension loading is not avoidable. Stress softening is an important phenomenon occurring in all elastomeric materials under cyclic tension loading. This research has experimentally investigated stress-strain characteristics, permanent set strain and hysteresis loss energy of the thin monoholar rubber flat slab in comparison with the thin solid rubber fat slab when undergoing 7 cycles of stretching. Results show noticeable differences in stress-strain hysteresis loops diminution of the thin monoholar rubber flat slab and the solid rubber flat slab. However, the difference in stress softening is not so pronounced. Only discernible differences can be observed in the 2nd to 5th loading cycles. Permanent set strain and diminution of hysteresis loss energy of the monoholar rubber flat slab specimens are clearly larger than that of the solid rubber flat slab. The monoholar rubber flat slab is thus more susceptible to damage and has greater reduction in elastic stiffness. Therefore stress softening may not be a matter of great concern when the monoholar rubber flat slab is adopted in practical applications provided both permanent set strain and hysteresis loss energy have been properly accounted for.

Acknowledgements

The authors are thankful to the Rubber and Polymer Technology Program, Faculty of Science and Technology Songkhla Rajabhat University for materials, tools, equipment and space for the experiment. Financial support for this research from Faculty of Engineering, Pathumwan Institute of Technology is also greatly appreciated.

References

[1] C. Yanyu, J. Zian, and W. Lifeng, "Hierarchical honeycomb lattice metamaterials with improved thermal resistance and mechanical properties," *Composite Structures*, vol. 152, pp. 395-402, 2016.

[2] C. Spadaccini, "Mechanical metamaterials: Design, fabrication, and performance," *National Laboratory under Contract* DE-AC52-07NA27344. 2015.

[3] B. Kulyuth, M. Chaiyoot, C. Suppachai, and M. Prapas, "Microstructure and hardness of friction welded SSM 356 aluminium alloy," *Advanced Materials Research*, vol. 887-888, pp. 1273-1279, 2014.

[4] G. Mario, and D. Laurent, "Impact & improvement of tool deviation in friction stir welding: Weld quality & real-time compensation on an industrial robot," *Robotics and Computer-Integrated Manufacturing*, vol. 39, pp. 22-31. 2016.

[5] Y. Liu, A. Li n, X. Cheng, S. Q. Zhang, and H. M. Wang, "Effects of heat treatment on microstructure and tensile properties of laser melting deposited AISI 431 martensitic stainless steel," *Materials Science & Engineering*, vol. A666, pp. 27-33, 2016.

[6] M. J. Morales-Conde, C. Rodriguez-Linan, and M. A. Pedreno-Rojas, "Physical and mechanical properties of wood-gypsum composites from demolition material in rehabilitation works," *Construction and Building Materials*, vol. 114, pp. 6-14, 2016.

[7] B. Md. Masum, K. Raisuddin, and A. S. Amir, "SMARS-I: Smart material actuated robotic snake (Ver-1)," *Science Direct*, vol. 3, pp. 572-577, 2016.

[8] B. Florijn, C. Coulaisab, and M. V Heckeab, "Programmable mechanical metamaterials: the role of geometry," *The Royal Society of Chemistry*, vol. 42, pp. 8736-8743, 2016.

[9] B. Florijn, C. Coulaisab and M. V. Heckeab, "Programmable mechanical metamaterials," *Physical Review Letters*, vol. 113, pp. 17-24, 2014.

[10] T. Mullin, S. Deschanel, K. Bertoldi, and M. C. Boyce, "Pattern transformation triggered by deformation," *Physical Review Letters*, vol. 99, pp. 084301, 2007.

[11] K. Bertoldi, M. Boyce, S. Deschanel, and S. Prange, "Mullin T. Mechanics of deformation-triggered pattern transformations and superelastic behavior in periodic elastomeric structures," *Journal of the Mechanics and Physics of Solids*, vol. 56, pp. 2642, 2008.

[12] K. Bertoldi, P. M Reis, S. Willshaw, and T. Mullin, "Negative Poisson's ratio behavior induced by an elastic instability," *Advanced Materials*, vol. 22, pp. 361, 2010.

[13] J. T. B. Overvelde, S. Shan, and K. Bertoldi, "Compaction through buckling in 2D periodic, soft and porous structures: effect of pore shape," *Advanced Materials*, vol. 24, pp. 2337, 2012.

[14] Y. Chen, Z. Jia, and L. Wang, "Hierarchical honeycomb lattice metamaterials with inproved themal resistance and mechanical properties," *Composite structures*, vol.152, pp. 395-402, 2016.

[15] A. A. Zadpoor, "Mechanical meta-materials," *The royal Society of chemistry*, vol. 3, pp. 371-381, 2016.

[16] K. Boonseng, C. Waiyapattanakorn, and P. Surin. "Notable mechanical behavior of thin monoholar rubber flat slab under tension loading," *Engineering and Applied Science Research*, vol. 48, no. 1, pp. 1-7, 2021.

[17] L. J. Gibson, and M. F. Ashby, "*Cellular solids: structure and properties. 2nd ed*. Cambridge University Press, U.K, 1997.

[18] K. Zhang, X. W. Zhao, H. L. Duan, B. L. Karihaloo, and J. Wang, "Pattern transformations in periodic cellular solids under external stimuli," *Journal of Applied Physics*, vol. 109 pp. 084907, 2011.

[19] T. Mullin, S. Deschanel, K. Bertoldi, and M. C. Boyce, "Pattern transformation triggered by deformation," *Journal of Physical Review Letters*, vol. 99, pp. 084301, 2007.

[20] K. Bertoldi, and M. C. Boyce, "Mechanically triggered transformations of phononic band gaps in periodic elastomeric structures," *Journal of Physical Review*, vol. 77, pp. 052105, 2008.

[21] H. M. A. Kolken, and A. A. Zadpoor, "Auxetic mechanical metamaterials," *The Royal Society of Chemistry*, vol. 7, pp. 5111-5129, 2017.

[22] X. Yu, J. Zhou, H. Liang, Z Jiang, and L. Wu, "Mechanical metamaterials associated with stiffness rigidity and compressibility: A brief review," *Progress in Materials Science*, vol. 94, pp. 114-173, 2018.

[23] Z. G. Nicolaou1, and A. E. Motter, "Mechanical metamaterials with negative compressibility transitions," *Nature Materials*, vol. 11, pp. 608-613, 2012.

[24] C. L. Kane, and T. C. Lubensky, "Topological boundary modes in isostatic lattices," *Nature Physics*, vol. 10, pp. 39-45, 2014.

[25] J. T. B. Overvelde, S. Shan, and K. Bertoldi, "Compaction through buckling in 2D periodic, soft and porous structures: effect of pore Shape," *Advance Material*, vol. 24, pp. 2337-2342, 2012.

[26] M. Sanami, N. Ravirala, K. Alderson, and A. Alderson, "Auxetic materials for sports applications," *Procedia Engineering*, vol. 72, pp. 453-458, 2014.

[27] M. Bianchi, F. Scarpa, and C. Smith, "Shape memory behavior in auxetic foams: Mechanical properties," *Acta Materialia*, vol. 58, no. 3, pp. 858-865, 2010.

[28] C. Lira, F. Scarpa, and R. Rajasekaran, "A gradient cellular core for aeroengine fan blades based on auxetic configurations," *Journal of Intelligent Material Systems and Structures*, vol. 22, no. 9, pp. 907-917, 2011.

[29] Q. Liu, "Literature review: Materials with negative Poisson's ratios and potential applications to aerospace and defence," *DTIC Document*, 2006.

[30] L. Santo, "Shape memory polymer foams," *Progress in Aerospace Sciences*, vol. 81, pp. 60-65, 2016.

[31] N. Phuhiangpa, W. Ponloa, S. Phongphanphanee, and W. Smitthipong, "Performance of nano- and microcalcium carbonate in uncrosslinked natural rubber composites: New results of structure–properties relationship," *Polymers*, vol. 12, no. 9, pp.1-15, 2020.

[32] A. E. Zuniga, A. L.M. Palacios-Pineda, I. A. Perales-Martinez, O. Martinez-Romero, D. Olvera-Trejo, and I.H. Jimenez-Cedeno, "Investigating the mullins effect and energy dissipation in magnetorheological polyurethane elastomers," *International Journal of Molecular Sciences*, vol. 21, no. 15, pp.1-24, 2020.

[33] M. Qian, B. Zou , Z. Chen, W. Huang, X. Wang, B. Tang, Q. Liu, and Y. Zhu, "The influence of filler size and crosslinking degree of polymers on mullins effect in filled NR/BR composites," *Polymers (Basel)*, vol.13, no. 14, pp.1-16, 2021.

[34] J. Diani, B. Fayolle, and P. Gilormini, "A-review-on-the-Mullins-effect," *European Polymer Journal*, vol. 45, pp. 601-612, 2009.

[35] L. Mullins, "Effect of stretching on the properties of rubber," *Journal of Rubber Research*, Vol. 16, pp. 275-289, 1947.

[36] S. Cantournet, R. Desmorat, and J. Besson, "Mullins effect and cyclic stress softening of filled elastomers by internal sliding and friction thermodynamics model," *International Journal of Solids and Structures*, vol. 46, pp. 2255-2264, 2009.

[37] S. Govindjee, and J. C. Simo, "A micro-mechanically based continuum damage model for carbon black-filled rubbers incorporating Mullin's effect," *Journal of the Mechanics and Physics of* Solids, vol. 39, pp. 87-112, 1991.

[38] L. Mullins, "Softening of rubber by deformation," *Rubber Chemistry and Technology*, vol. 42, pp. 339-362, 1969.

[39] L. Mullins, "Permanent set in vulcanized rubber" *India Rubber World*, vol. 120, pp. 63-66, 1949.